JAM CM Journal of Applied Mathematics and Computational Mechanics 2026, 25(1), 19-30
www.amcm.pcz.pl p-ISSN 2299-9965
DOI: 10.17512/jamcm.2026.1.02 e-ISSN 2353-0588

FOURIER TRANSFORM-BASED IDENTIFICATION OF SPECTRAL PROPERTIES OF NONLINEAR MECHANICAL SYSTEMS

Ján Minárik[1], Milan Sága[1], Milan Vaško[1], Branislav Ftorek[2], Tomasz Domański[3]

[1] Department of Applied Mechanics, University of Žilina, Žilina, Slovakia
[2] Department of Applied Mathematics, University of Žilina, Žilina, Slovakia
[3] Department of Mechanics and Machine Design, Czestochowa University of Technology Częstochowa, Poland
Jan.Minarik@fstroj.uniza.sk, Milan.Saga@fstroj.uniza.sk, Milan.Vasko@fstroj.uniza.sk
Branislav.Ftorek@fstroj.uniza.sk, tomasz.domanski@pcz.pl

Received: 24 September 2025; Accepted: 2 December 2025

Abstract. The article aims to study the spectral properties of oscillating mechanical systems that comprise hysteretic components. The authors modelled the treated hysteretic systems as systems of nonlinear differential equations and used the MATLAB environment to obtain the respective numerical solutions. The results were then transformed into the frequency domains using the Fourier transform. The corresponding linear system used as a reference was processed in the same manner. The frequency domains were then analyzed and compared in order to investigate the influence of hysteresis on the treated systems. The obtained results show that the hysteretic components have a considerable impact on the natural frequencies of the studied systems. These varied according to the changes in stiffness that are a natural result of the hysteresis.

MSC 2010: *70G08, 70K08*
Keywords: *hysteresis, natural frequency, Fourier transform, oscillations*

1. Introduction

The operation of machines is naturally accompanied by the occurrence of vibrations. The impact of vibrations is usually negative; furthermore, they can significantly influence the operation and reliability of machines. Therefore, the natural frequencies are important parameters of the mechanical systems. These frequencies should not interfere with the machine's operating frequencies. Otherwise, resonance can occur. This is an undesirable state that may result in machine destruction. Modal and spectral analyses represent the tools to determine the natural frequencies and respective normal modes of the mechanical systems. The results obtained by the analysis can be further used to modify or optimize the treated machine [1, 2].

Real components are flexible, with their natural frequencies and modes being determined by the distribution of their mass and stiffness. These components are often

modelled as linear, thus with constant stiffness. This approach is relatively simple, and the problem can be described using linear mathematical models. However, the characteristics of real components are often nonlinear, which might cause hysteretic effects. In such cases, simple linear models can no longer adequately describe the treated problem.

In mechanics, the hysteresis represents the nonlinear relationship between the loads and system responses. Moreover, this relationship becomes time-dependent. In this way, the mechanical systems exhibit memory effects, energy dissipation, and nonlinear behaviour in general. Hysteresis can be utilized in the modelling of various problems, such as material behaviour, suspension components, or various types of mechanical joints [3-5]. However, it is used to a large extent in other fields as well. As of now, a large number of mathematical models describing hysteresis have been proposed. As one of the most well-known and commonly used, the Bouc-Wen class models can be mentioned. These models are determined by a single differential equation of first order. This allows for a simple implementation of the models while offering relatively high flexibility of hysteretic loop shapes [6, 7]. The frequency response of hysteretic systems is treated in the following studies [8, 9].

The article analyses the influence of hysteresis on the natural frequencies of oscillators and their systems. The authors dealt with a 1 DOF hysteretic oscillator as well as with a 2 DOF system of oscillators coupled by a hysteretic spring. The aim of this study is to assess the impact of hysteresis, primarily in a qualitative manner. Thus, the selection of system parameters was not based on a specific real-world system. The behaviour of hysteretic components was described by the Bouc-Wen model. A total of six hysteretic loop shapes were analyzed: three exhibiting decreasing stiffness and three exhibiting increasing stiffness. Moreover, the reference linear models were treated as well. The oscillations of the systems were induced by the force with a time-varying frequency. The treated systems were modelled and solved using MATLAB. The results were then processed by the Fourier transform (FFT) to obtain the corresponding natural frequencies. The data provided by the hysteretic models were compared with those provided by the reference linear models. The authors then examined how the hysteresis influences the natural frequencies of the treated systems.

2. Problem statement

In the next sections, the treated problems are presented in detail. First, the case of a 1 DOF hysteretic oscillator is described. Next, the 2 DOF system of oscillators coupled by a hysteretic spring is presented. The hysteretic components are described by the Bouc-Wen models, using several hysteretic loop shapes.

2.1. 1 DOF oscillator

The treated problem is shown in Figure 1, which describes the hysteretic oscillator with 1 degree of freedom. The oscillator has a mass m with initial stiffness k.

Its hysteretic behavior is described by the hysteretic control function z. In this case, the damping is a result of hysteresis only. The oscillations are induced by the force $F(t)$ with a time-varying frequency, shown in Figure 2. The force has the form:

$$F(t) = A_F \cdot \sin[2\pi \cdot f(t)], \tag{1}$$

Here, A_F is the force amplitude, and the time derivative $\dot{f}(t) = 0.2 + 2.8t/t_2$ represents the time-dependent frequency that increases linearly with time, from 0.2 Hz at $t_1 = 0$, to 3 Hz at $t_2 = 40$ s [10]. Parameters t_1, t_2 denote the simulation start and end time. In this case, the authors assume the oscillator displacement reaches its maximum when the oscillator's natural frequency corresponds to the frequency of the driving force. The parameters of a linear model (k, m), as well as the driving force, were kept the same as in the hysteretic model. However, the linear system contains a viscous damper with a coefficient of damping b. The values of the parameters are as follows: $m = 1.5$ kg, $k = 180$ N/m, $b = 2.5$ kg/s and $A_F = 50$ N.

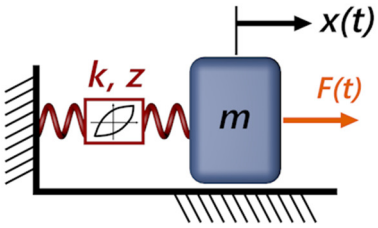

Fig. 1. Model of 1 DOF oscillator

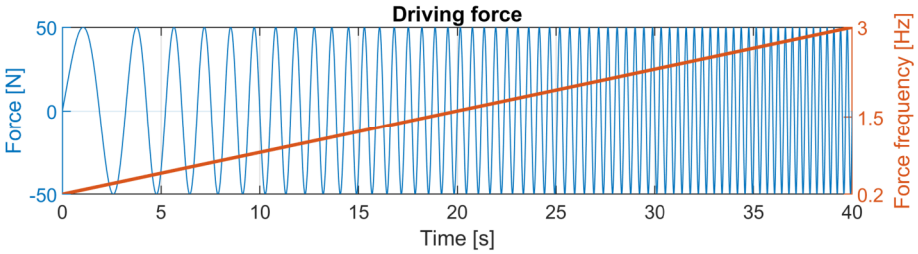

Fig. 2. Time course of the driving force $F(t)$

Considering the Bouc-Wen model, the hysteretic restoring force can be written in the following form:

$$F_h = \alpha k y + (1 - \alpha) k z. \tag{2}$$

Parameter α denotes the stiffness ratio, and y is the instantaneous displacement of the oscillator. The hysteretic loop shape is defined by the control function z. Prior to the solution, this function is only known in its differential form $\dot{z}(\dot{y}, z)$. This form provides an additional differential equation that has to be solved together with the equations of motion. The form of $\dot{z}$ for the Bouc-Wen model is given as:

$$\dot{z}(\dot{y}, z) = \{A - |z|^n[\,\gamma + \beta \mathrm{sgn}(\dot{y}z)]\}\dot{y}. \tag{3}$$

The constant A influences the initial loop slope, and n controls the loop sharpness. The sum and difference of the constants β and γ then define the resulting loop shape. The authors utilized six loop shapes in total: three, denoted as *type A*, with decreasing stiffness, and three, denoted as *type B*, with increasing stiffness. The sums and differences of constants β and γ are stated in Table 1. The values of $\alpha = 0.1$ and $A = 1$ were the same for each loop.

Table 1. The parameters of hysteretic loops

	Decreasing stiffness			Increasing stiffness		
Loop	A1	A2	A3	B1	B2	B3
$\gamma + \beta$	0.30	0.60	0.90	–0.30	–0.60	–0.90
$\gamma - \beta$	–0.45	–0.01	0.42	–1.10	–1.46	–1.82

The sum $\gamma + \beta$ defines the change in a loop slope, and thus the change in stiffness, during loading. Positive values then correspond to the increase and negative values to the decrease of stiffness. The rate of change in stiffness then increases with an increasing absolute value of the sum. The difference $\gamma - \beta$ then describes the loop slope change during unloading. These values were selected such that the standard deviation (SD) of the oscillator displacement is approximately the same for both hysteretic and linear models. The purpose of this requirement was to achieve statistically equivalent behaviour of the oscillators.

In the case of a linear model, the equation of motion has the form $m\ddot{y} + b\dot{y} + ky = F(t)$. For the hysteretic models, we consider the hysteretic force (2). Together with the additional differential equation (3), the equations of motion of the oscillator then have the form:

$$\begin{aligned} m\ddot{y} &= -\alpha k y - (1-\alpha)kz + F(t), \\ \dot{z} &= \{A - |z|^n[\gamma + \beta \mathrm{sgn}(\dot{y}z)]\}\dot{y}. \end{aligned} \tag{4}$$

The linear damping component $b\dot{y}$ is not considered in hysteretic models. Energy dissipation is thus solely a result of hysteresis. Using the substitutions $y = y_1$ and $\dot{y} = y_2$, the system (4) was transformed into a space state system and then solved in MATLAB, with the use of the built-in ODE45 solver, which is based on the Runge-Kutta (4.5) method. This solver utilizes an adaptive time step, governed by the relative error tolerance, which was set to 10^{-6}. At each time step, this value multiplies the magnitude of each solution component to obtain the respective error tolerances [11]. The solution was obtained for the time $t \in \langle 0; 40 \rangle$ s, with the initial conditions $y_1(0) = \dot{y}_1(0) = y_2(0) = \dot{y}_2(0) = z(0) = 0$.

2.2. 2 DOF system of oscillators

The treated problem is shown in Figure 3. The system comprises two weights of masses m_1 and m_2. The weights are attached to the moving frame by two linear springs with constant stiffnesses k_1 and k_2. The system also contains two viscous dampers with the coefficients of damping b_1 and b_2. The weights are coupled by a hysteretic spring with an initial stiffness k_3. The hysteretic behaviour is given by the hysteretic control function z. The instantaneous displacements of the weights are denoted $x_1(t)$ and $x_2(t)$.

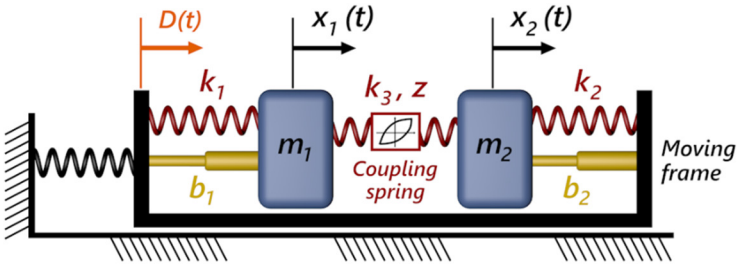

Fig. 3. 2 DOF system of coupled oscillators

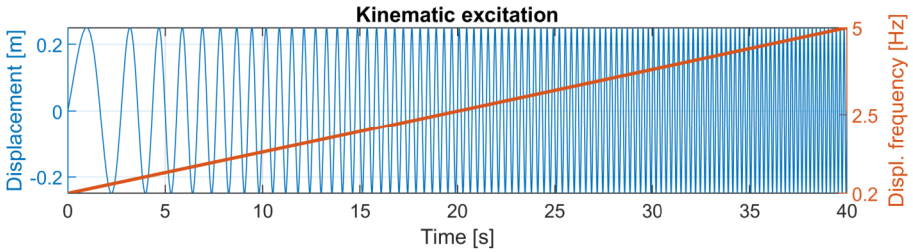

Fig. 4. Kinematic excitation function $D(t)$

The oscillation of the system is induced by the motion of the frame, which is given by the kinematic excitation function of the form $D(t) = A_X \cdot \sin[2\pi \cdot f(t)]$. This function is shown in Figure 4. The meaning of the presented parameters is analogous to the previous case. The constant A_X describes the amplitude of oscillations, and the time derivative $\dot{f}(t) = 0.2 + 4.8t/t_2$ again represents the time-varying frequency that increases linearly from 0.2 Hz at the simulation start time $t_1 = 0$ to 5 Hz at the simulation end time $t_2 = 40$ s. Again, the authors assume that the displacements will reach their maximum values when the driving frequency reaches any of the system's natural frequencies.

The parameters of the reference linear model and the hysteretic model have the same values. This holds for the kinematic excitation function as well. However, in the linear case, the hysteretic characteristics are replaced by the constant stiffness k_3 and a damper with a coefficient of viscous damping b_3. The system parameters have the following values: $k_1 = 90$ N/m, $k_2 = 355$ N/m, $k_3 = 100$ N/m, $b_1 = 1.25$ kg/s, $b_2 = 0.15$ kg/s, $b_3 = 1.00$ kg/s and $A_X = 0.25$ m.

Again, a total of six loop shapes were utilized: three hysteretic loops described the decrease of stiffness (*type A*) and three described the increase of stiffness (*type B*). The hysteretic loops were modelled using the Bouc-Wen model, given by equations (2) and (3). Sums $\gamma + \beta$ and differences $\gamma - \beta$, determining the loop shapes, are given in Table 2.

Table 2. Hysteretic loops parameters

	Decreasing stiffness			Increasing stiffness		
Loop	A1	A2	A3	B1	B2	B3
$\gamma + \beta$	0.30	0.60	0.90	0.30	–0.60	–0.90
$\gamma - \beta$	–0.61	–0.38	–0.20	–1.10	–1.40	–1.68

The values $\gamma - \beta$ were selected such that the SDs of the coupling spring displacements are approximately the same for each model. The values of $\alpha = 0.1$ and $A = 1$ were the same for all the loop shapes.

Considering the hysteretic force (2), as well as the hysteretic control function (3), the equations of motion can be written as:

$$\begin{aligned} m_1\ddot{x}_1 &= k_1[\mathrm{D}(t) - x_1] + \alpha k_3(x_2 - x_1) + (1-\alpha)k_3 z, \\ m_2\ddot{x}_2 &= k_2[\mathrm{D}(t) - x_2] - \alpha k_3(x_2 - x_1) - (1-\alpha)k_3 z, \\ \dot{z} &= \left\{ A - |z|^n \left[\gamma + \beta \mathrm{sgn}\left((\dot{x}_2 - \dot{x}_1) z\right) \right] \right\} (\dot{x}_2 - \dot{x}_1). \end{aligned} \tag{5}$$

In the case of a linear model, $\alpha = 1$ with the hysteretic terms $\pm(1-\alpha)k_3 z$ being replaced by the damping forces $\pm b_3(\dot{x}_2 - \dot{x}_1)$. These are not present in the hysteretic model. After discarding the hysteretic terms, the hysteretic control function z becomes obsolete. Therefore, it is not solved as part of the linear model. Using the substitutions $x_1 = \chi_1$, $\dot{x}_1 = \mathrm{X}_1$, $x_2 = \chi_2$, $\dot{x}_2 = \mathrm{X}_2$, the system (5) was transformed to a system of 5 differential equations of the first order (4 equations in the case of the linear model). As in the previous case, the system was solved in MATLAB, using the ODE45 solver. The results were for the time $t \in \langle 0; 40 \rangle$ s and for the initial conditions $\chi_1(0) = \mathrm{X}_1(0) = \chi_2(0) = \mathrm{X}_2(0) = z(0) = 0$.

3. Results

The next section presents the obtained results. These comprise the solutions of the equations of motion as well as the corresponding FFTs. The FFTs were used to determine the natural frequencies of the treated systems. The hysteretic loops, representing the relationship between the restoring force and displacement of the hysteretic component, are also presented.

3.1. 1 DOF oscillator

The solutions in the time domain and the corresponding FFTs for the systems with decreasing stiffness are shown in Figure 5. The loop shapes are denoted $A1$ to $A3$ and are shown in Figure 6. The results for the case of increasing stiffness are shown in Figure 7, with the corresponding loop shapes being presented in Figure 8. These are denoted $B1$ to $B3$. All the hysteretic loops have the same initial stiffness corresponding to the value k_3 (Figs. 6, 8).

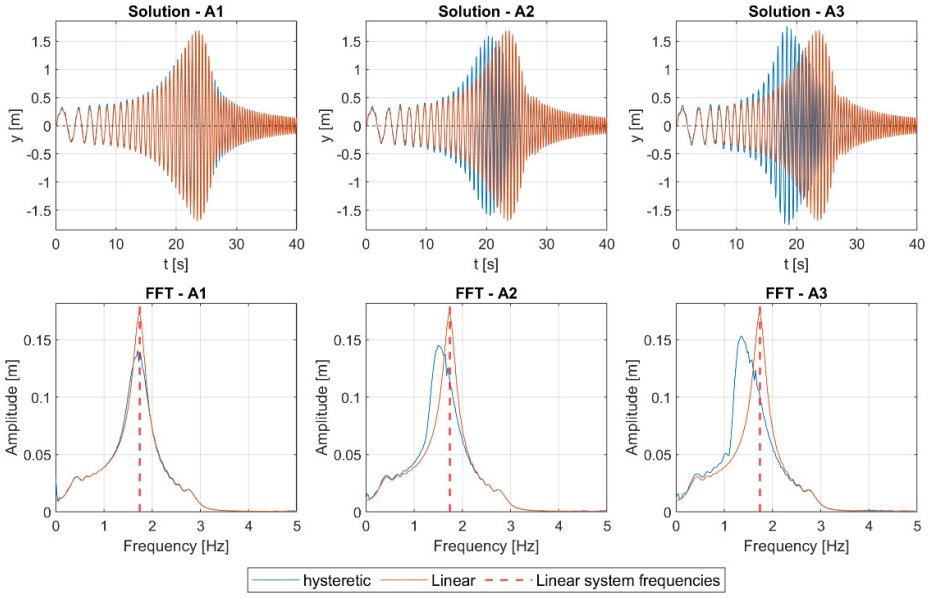

Fig. 5. The solutions in the time domain (top) and the corresponding FFTs (bottom) for the models with decreasing stiffness

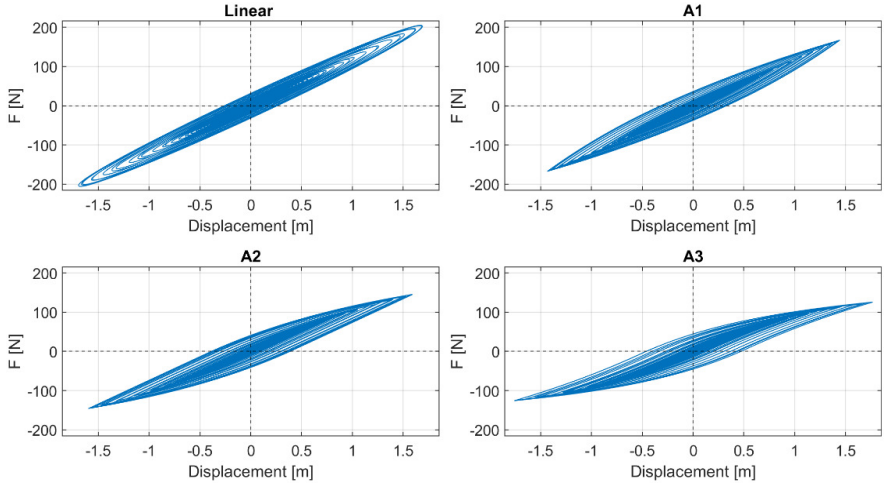

Fig. 6. Hysteretic loops with increasing stiffness

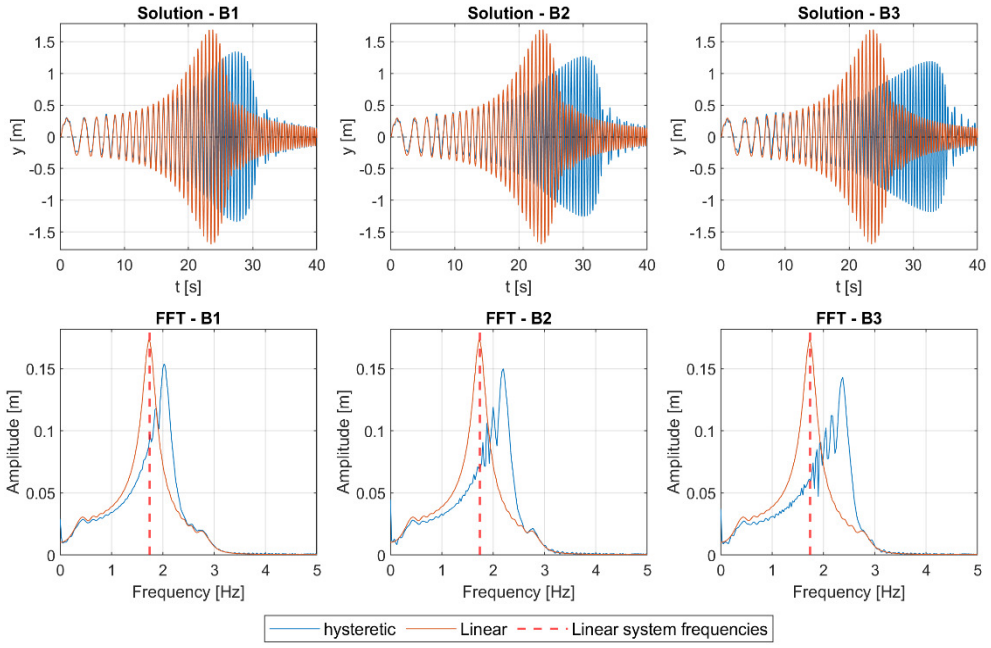

Fig. 7. Solutions in the time domain (top) and the corresponding FFTs (bottom) for the models with increasing stiffness

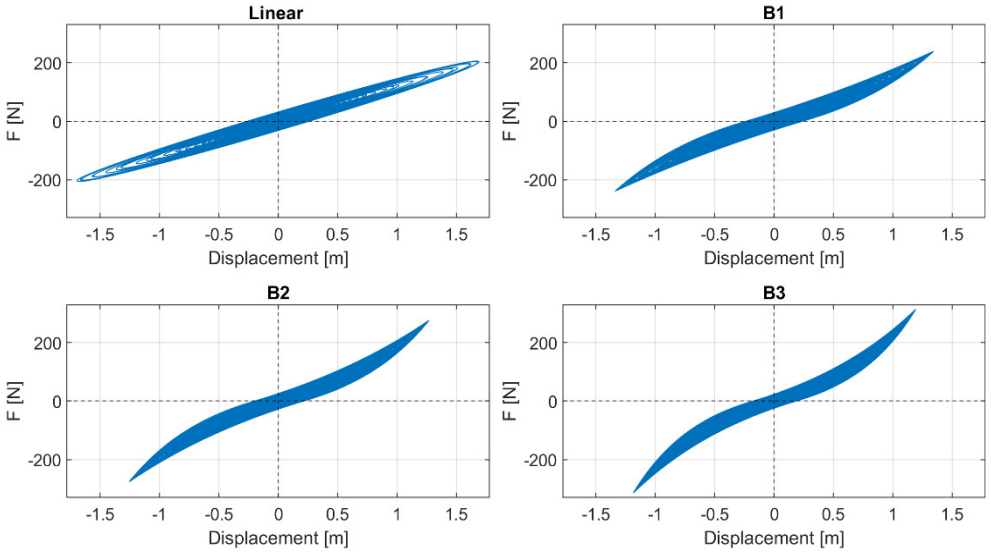

Fig. 8. Hysteretic loops for the models with increasing stiffness

Considering the *type A* models, the loop with the lowest decrease in stiffness is denoted as *A*1, and the loop with the highest decrease is denoted *A*3. The presented FFTs show that hysteresis caused the decrease of natural frequencies. This decrease

is more distinct for loops with greater stiffness change. The solutions in the time domain demonstrate this phenomenon as well. The hysteretic systems reach maximum displacement before the linear system, when the driving force frequency is lower. Furthermore, this is accompanied by a slight increase in maximum displacements.

The results provided by *type B* models are similar to those in the previous case. Again, $B1$ denotes the loop with the lowest change in stiffness, while $B3$ denotes the loop with the highest change in stiffness. In this case, the hysteresis caused an increase in natural frequencies. The increase is more distinct for loops with greater stiffness change. The FFTs also show peaks appearing at frequencies lower than the natural frequencies. This might be caused by the sharp change of stiffness when the loading direction changes, or naturally by the varying oscillator stiffness. Similar behaviour can also be seen in the previous case, but to a significantly lower extent. The results provided by the FFTs can be observed in the time domain as well. The maximum displacements of the hysteretic models appear after the linear model, when the driving force frequency is higher. Additionally, a slight decrease in maximum displacements can be noticed.

3.2. 2 DOF system of oscillators

The results for the case of decreasing stiffness are depicted in Figure 9. The figures show the displacements of each body, the corresponding FFTs, and the hysteretic loops describing the forces in the coupling spring. The individual loop shapes are denoted $A1$ to $A3$. The results for models with increasing stiffness are then shown in Figure 10. These loop shapes are denoted $B1$ to $B3$. The obtained results show that the behaviour of 2 DOF systems is generally similar to that of 1 DOF oscillator. The initial stiffness was the same for all hysteretic loops.

In the case of decreasing stiffness, the loop $A1$ possesses the lowest and $A3$ the highest decrease. The FFTs show that the hysteresis causes both natural frequencies to decrease, which can be attributed to the reduction of system stiffness. The change in natural frequency is more noticeable for loops describing greater change in stiffness. Furthermore, it can be observed that the change in the second natural frequency is more distinct. This behavior is noticeable in the time domain as well. The maximum displacements of hysteretic systems occur slightly sooner, compared to those in the linear model.

The behaviour of the system with increasing stiffness is also analogous to the 1 DOF oscillator. Again, $B1$ describes the lowest and $B3$ the highest increase in stiffness. In this case, the FFTs show that the hysteresis causes an increase in both the natural frequencies, which is more distinct for loops with greater stiffness. The second natural frequency changes more noticeably, with additional lower peaks appearing at frequencies below the shifted peak. The change in natural frequencies is also evident in the time domain, particularly in the case of the second body displacement.

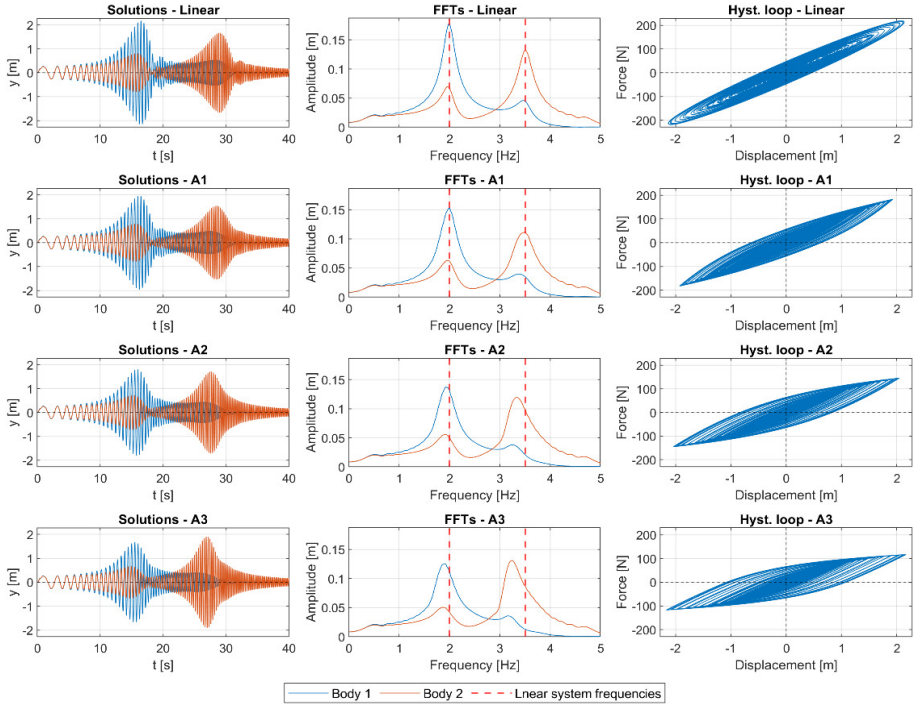

Fig. 9. Results for the system with decreasing stiffness

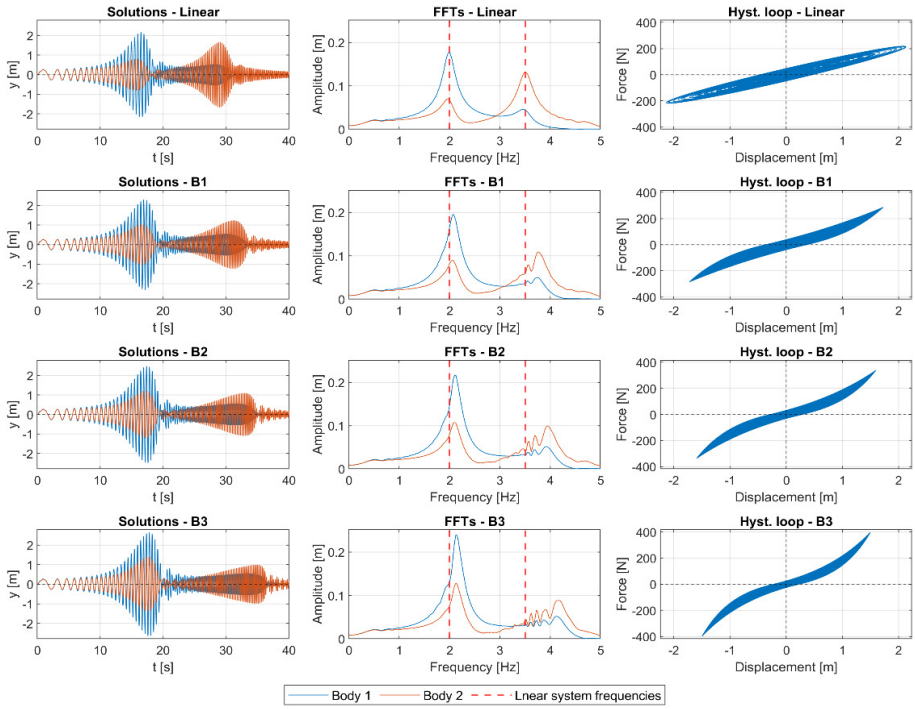

Fig. 10. Results for the system with increasing stiffness

4. Conclusion

The article studied the influence of hysteretic components on the frequency response of the oscillators and their systems. The treated models comprise hysteretic springs described by the well-known Bouc-Wen model. Several hysteretic loop shapes were utilized, with both decreasing as well as increasing stiffness. Natural frequencies were determined by the FFTs of the obtained solutions. All the presented problems were modelled in MATLAB.

The results showed that hysteresis influences the frequency spectrum of both 1 DOF oscillators as well as their 2 DOF systems. In both cases, the hysteresis manifests itself in an analogous way. Hysteretic loops with decreasing slopes are likely to reduce the stiffness of the system, thus resulting in a decrease in natural frequencies. On the contrary, the loops with increasing slopes resulted in increased natural frequencies. In general, the results showed that the change in natural frequencies is more distinct for loops with greater slope change. The presented phenomena occurred regardless of whether it was a 1 DOF oscillator or a 2 DOF system. Thus, the hysteretic components can influence the frequency response of the mechanical systems in various ways and to various extents. This is because hysteresis characterizes the stiffness and the damping of the system. Therefore, the properties of hysteretic components can be utilized, for example, in spectral tuning of mechanical systems.

Acknowledgements

This work was supported by the projects VEGA, No. 1/0423/23, and KEGA, No. 005ŽU-4/2024.

References

[1] Grega, I., Grega, R., & Homišin, J. (2021). Frequency of free vibration in systems with a power-law restoring force. *Bulletin of the Polish Academy of Sciences, Technical Sciences*, *69*(2), e136723. DOI: 10.24425/bpasts.2021.136723.

[2] Yang, Ch., Li, Q., & Chen, Q. (2021). Natural frequency analysis of parallel manipulators using global independent generalized displacement coordinates. *Mechanism and Machine Theory*, *156*, 104145. DOI: 10.1016/j.mechmachtheory.2020.104145.

[3] Halama, R., Fusek, M., & Poruba, Z. (2016). Influence of mean stress and stress amplitude on uniaxial and biaxial ratcheting of ST52 steel and its prediction by the Abdel-Karim-Ohno model. *International Journal of Fatigue*, *91*(2), 313-321. DOI: 10.1016/j.ijfatigue.2016.04.033.

[4] Bartošák, M., Horváth, J., & Španiel, M. (2021). Multiaxial low-cycle thermo-mechanical fatigue of a low-alloy martensitic steel: Cyclic mechanical behaviour, damage mechanisms and life prediction. *International Journal of Fatigue*, *151*, 106383. DOI: 10.1016/j.ijfatigue.2021.106383.

[5] Hua, C.R., Zhao, Y., & Ouyang, H. (2018). Random vibration of vehicle with hysteretic nonlinear suspension under road roughness excitation. *Advances in Mechanical Engineering*, *10*(1). DOI: 10.1177/1687814017751222.

[6] Wang, T. et al. (2023). From model-driven to data-driven: A review of hysteresis modeling in structural and mechanical systems. *Mechanical Systems and Signal Processing*, *204*(1), 110785. DOI: 10.1016/j.ymssp.2023.110785.

[7] Ismail, M., Ikhouane, F., & Rodellar, J. (2009). The hysteresis Bouc-Wen model, a survey. *Archives of Computational Methods in Engineering*, *16*, 161-188. DOI: 10.1007/s11831-009-9031-8.

[8] Casini, P., & Vestroni, F. (2018). Nonlinear resonances of hysteretic oscillators. *Acta Mechanica*, *229*, 939-952. DOI: 10.1007/s00707-017-2039-5.

[9] Vestroni, F., & Casini, P. (2020). Mitigation of structural vibrations by hysteretic oscillators in internal resonance. *Nonlinear Dynamics*, *99*(11), 505-518. DOI: 10.1007/s11071-019-05129-9.

[10] Tuan, L., V., Korotina, M., Bobtsov, A., Aranovskiy, S., & Pyrkin, A. (2019). Online estimation of time-varying frequency of a sinusoidal signal. *IFAC-PapersOnLine*, *52*(29), 245-250. DOI: 10.1016/j.ifacol.2019.12.657.

[11] Mathworks. ODE45. Available online: https://www.mathworks.com/help/matlab/ref/ode45/ [cited: 5.7.2025].